Examining the Thermal Degradation Behaviour of a Series of Cyanate Ester Homopolymers

S. Gouthaman[a], M. Venkatesh[a], S.O. Kanemoto[a,b], M. Suguna Lakshmi[a], I. Hamerton[c*]

[a] *Polymer Science & Technology Division, Central Leather Research Institute (CSIR – CLRI), Chennai, 600 020, India.*

[b] *Macromolecular Research Team, Department of Inorganic Chemistry, University of Yaounde-I, 812-Yaounde, Cameroon.*

[c] *Bristol Composites Institute (ACCIS), Department of Aerospace Engineering, School of Civil, Aerospace, and Mechanical Engineering, Queen's Building, University of Bristol, University Walk, Bristol, BS8 1TR, U.K.*

Abstract

A series of thermally stable dicyanate monomers, containing different thermally stable structural units, *viz* 2,2'-*bis* (4-cyanatophenyl)propane (DCDPP), *bis*-4-cyanato-biphenyl (DCBP), *bis*-4-cyanato naphthalene (DCN), 3,3'-*bis*(4-cyanatophenyl) sulphide (DCTDP) and 3,3'-*bis* (4-cyanatophenyl) sulphone (DCDPS), is prepared and the identity of the products confirmed by FT-IR and NMR spectral methods. The corresponding cyanate homopolymers (designated by the suffix HP) are prepared and their properties evaluated and compared. The composites were analysed for their thermal stability and thermal degradation kinetics. The series of homopolymers exhibit excellent thermal characteristics *e.g.* relatively high glass transition temperatures of at least 215 ºC, which were inversely proportional to the molecular weight between the crosslinks, high thermal decomposition temperature, high integral procedural decomposition temperature (IPDT), and high activation energies for the decomposition of the cured resins. Determination of their limiting oxygen indices indicates that all the homopolymers are characterized as 'self-extinguishing' materials.

KEY WORDS: *Cyanate esters, Homopolymers, Curing, Flame retardance, Thermogravimetric analysis*

*Prof. I. Hamerton, e-mail: ian.hamerton@bristol.ac.uk, Tel.: +44 (0)117 3314799

1. INTRODUCTION

Cyanate ester resins have stimulated substantial interest, due to their exclusive combination of properties, such as low water absorption, low dielectric constant and heat release rate, superior strength, excellent bonding towards metals, glass and carbon matrices, low volatility while curing, and high resistance towards high heat and high humid environments. Owing to their excellent final cured properties, they find application as structural adhesives for making high temperature resistant and light-weight advanced composites [1,2]. Cyanate esters have definite advantages over bismaleimide (BMI) resins due to lower typical crosslink densities and higher flexibility because of the high percentage of oxygen linkages present [3]. These attributes of cyanate esters are reflected in the higher fracture toughness observed when incorporated into epoxy resins in comparison with BMIs [4].

Cyanate ester resins are primarily used in the field of aerospace materials, in dielectric components, printed circuit boards, coatings and other applications requiring high temperature resistant and moisture resistant materials. These applications are the consequence of their high mechanical strength, high moisture resistance, low dielectric loss, low volatility during the cure, and low toxicity [5-6]. In recent years, many new cyanate monomers have emerged especially the dicyanates containing aromatic ether [7], ketone [8,9], 2,7-dihydroxynaphthalene [10], polyurethane [11], thiophenols [12,13], silicones [14,15] and phosphorus [16,17]. Though cyanate esters are known to exhibit excellent thermal properties, investigations into the thermal behaviour, thermal stability and thermal degradation kinetics studies using different mathematical models under non-isothermal and isothermal conditions are more limited beyond very basic cyanate esters [18,19]. The trend for increased use of cyanate esters is due to the

growing demand for light-weight, low dielectric loss, high heat resistant structures for manufacturing military aircraft [4,20-27]. Consequently, in this study, a detailed and systematic evaluation is analyzed and discussed, especially concerning the thermal properties of the homopolymers.

2. MATERIALS AND METHODS

2.1. Materials

2,2-*Bis*(4-hydroxyphenyl)propane (99%), 1,4-naphthalene diol (99%), 4,4′-biphenyldiol (97%), 4,4'-thiodiphenol (99%), 4,4'-sulphonyl diphenol (98%), and cyanogen bromide (99%) were purchased from Aldrich Chemical Company. Triethylamine, acetone and methanol (Analytical Reagent grade) were purchased from S.D. Fine Chemicals Pvt. Ltd., Mumbai, India.

2.2. Synthesis of 2,2'-*bis*(4-cyanatophenyl)propane (DCDPP)

A batch scale of cyanate ester (100g) was synthesized at 0 °C by the reaction of cyanogen bromide (74.6 g, 0.7 mol.) and bisphenol A (81 g, 0.35 mol.). Triethylamine (90 g, 0.89 mol.) was added to catalyse the reaction and to absorb the evolved HBr to yield salts of tri-ethylamine hydrobromide (Fig. 1 and Fig. S1). The synthesis was carried out in a three-necked round-bottomed flask equipped with a mechanical stirrer and a nitrogen inlet was charged a cooled solution of bisphenol A and cyanogen bromide in acetone. Triethylamine was added dropwise under continuous stirring in an ice bath and, after complete addition, the reaction mixture was stirred for a further period of one hour while maintaining the ice bath temperature at 0 °C and filtered under vacuum. The reaction mixture was filtered and, the filtrate was poured into a large amount of cold distilled water (1L) to precipitate the bisphenol A cyanate ester, DCDPP, Fig 1(a), from the solution. The crude product was further purified by recrystallization in methanol: water (1:1 V/V). The product was a white crystalline with 76 g yield (80%) and m.p. 75-78 °C.

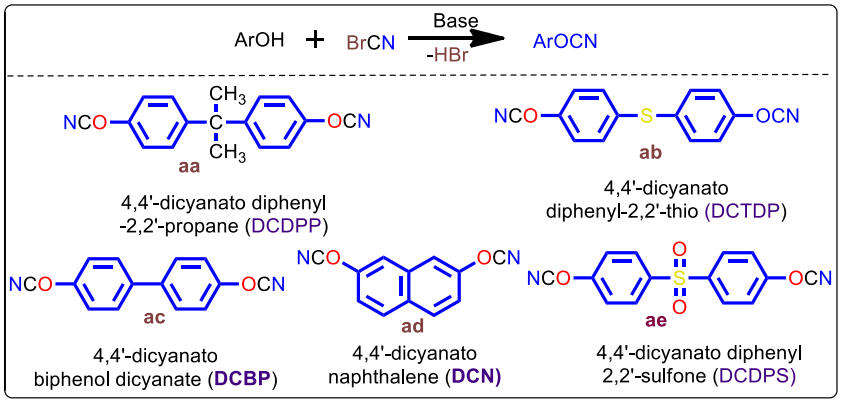

Fig. 1. Reaction scheme for the preparation of the dicyanate monomers (a-e).

The remaining cyanates: DCTDP (RMM 268; m.p. 79 °C solid, white colour), Fig 1(b), DCBP (RMM 236; m.p. 82 °C solid, brown colour), Fig 1(c), DCN (RMM 210; m.p. 80 °C, solid, dark brown colour), Fig 1(d), and DCDPS (RMM 300; m.p. 81 °C, solid, light brown colour), Fig 1(e) were prepared from their respective dihydroxy compounds by employing the same procedure [19,20]. All the products were characterized by FT-IR and ^{13}C NMR spectroscopic techniques. Each cyanate ester (100 parts) was homopolymerized (Fig. 2) by heating at 140 °C for 3 h, 160 °C for 2 h and followed by a post-curing at 180°C for 4h and 200 °C for 2 h.

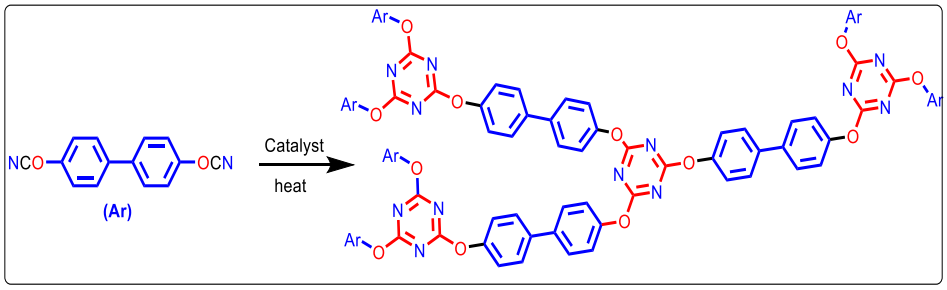

Fig. 2. General reaction scheme for the cyclotrimerisation of the dicyanate monomers.

2.3. Characterisation

Fourier Transform Infrared (FT-IR) spectra were obtained using a Nicolet model 20DXB spectrophotometer with KBr pellets for solid specimens within scanning range of 400-4000 cm^{-1} at the resolution of < 0.1 cm^{-1}. A JOEL ECA-500 nuclear magnetic resonance (NMR) spectrometer was used to carry out the analyses at 298K using TMS standard and $CDCl_3$ solvent. ^1H NMR spectra were recorded at 500 MHz and ^{13}C NMR at 125 MHz. The thermal stabilities of the cured polymers were determined using TGA Q50-TA thermal analyzer. The thermogravimetric analysis (TGA) curves were recorded between 30-800 °C for cured HP samples (10-15 mg) at a heating rate of 10°C/min and under a flowing nitrogen atmosphere (10 cm^3/min). The differential scanning calorimetric (DSC) studies were conducted on DSC Q200 TA instrument at the heating rate of 5 °C/min between 0-300 °C. Nitrogen gas flow rate was kept at the rate of 10 cm^3/min. Scanning electron microscopic (SEM) analysis was performed using a JEOL 400 microscope on the fractured surface of the cured neat resin applying an accelerating voltage of 5kV; the fractured samples were first sputtered with carbon.

3. RESULTS AND DISCUSSIONS

3.1. Characterization of monomers by FT-IR and ^{13}C NMR spectroscopy

FT-IR spectra of the dicyanate monomers (see Supplementary data, Fig. S2) display the characteristic (O-C≡N) doublet around 2200 cm^{-1}, confirming the presence of the cyanate group, while the ^{13}C NMR spectra (Fig. S3) showed the resonances corresponding to the cyanate functional groups and all the carbons present in the compounds. The characteristic signals of the OCN carbons attached to the aromatic rings for DCDPP, DCBP, DCN, DCTDP, and DCDPS were observed at 116, 109.4, 116.9, 106.5, and 111.6 ppm respectively. The aromatic carbons appeared in the range 129-188 ppm for DCBP, 118-153 ppm for DCDPP, 118-162 ppm for DCDPS, 106-154 ppm for DCN, and 116-156 ppm for DCTDP respectively.

3.2. DSC analysis

3.2.1. Thermal behaviour

From the DSC curves (Fig. S4) of the cured samples of cyanate homopolymers systems, DCDPP-HP, DCBP-HP, DCN-HP, DCTDP-HP, and DCDPS-HP exhibited their glass transition temperatures (T_g) at 247, 215, 256, 253, and 215 °C respectively. The high T_g of the homopolymer systems (> 200 °C) is due to the presence of the triazine rings, formed by the cyanate monomers. Amongst the homopolymer systems, DCN-HP exhibits the highest T_g: the naphthalene moiety has a rigid, planar structure, which packs more readily through π-π stacking [21-22]. The mass loss occurred up to 130 ^oC is because of the elimination of solvent and moisture for purification of polymers. Thermal stability of DCDPP-HP shows the highest and DCN-HP shows lowest due to the fused naphthalene core. Mainly, DCDPP-HP and DCPPS-HP show higher resistance to heat because of the presence of sulfone and dimethyl propane groups and which contribute to the single degradation step. On the other hand, the remaining three homopolymers display two degradation steps: the first due to the single bond scissions and the second could be the pyrolysis of the cyanurate rings (380 ^oC- 420 ^oC). The mass loss occurred up to 130 ^oC is because of the elimination of solvent and moisture for purification of polymers. Thermal stability of DCDPP-HP shows the highest and DCN-HP shows lowest due to the fused naphthalene core.

3.2.2. Estimation of M_c

The estimation of the molecular weights between adjacent crosslinks (M_c) helps to understand the development of the physical network structure of the polymer since M_c is inversely proportional to the crosslink density. The latter is one of the vital structural parameters that aid knowledge of the influence of changes in the segmental motions, which are reflected in the mechanical properties of thermoset polymers. When the number of crosslink junctions increases,

the crosslink density increases and this to a concomitant increase in T_g. Hence, the relationship between T_g and M_c can also be correlated with the crosslink density of the polymer. The M_c values for the homopolymer systems presented in this article were estimated using an empirical equation 1 [23].

$$Mc = \frac{3.9\times10^{4}}{Tg - Tg^{0}} \quad (1)$$

T_g^0 is the glass transition temperature of the non-crosslinked polymer.

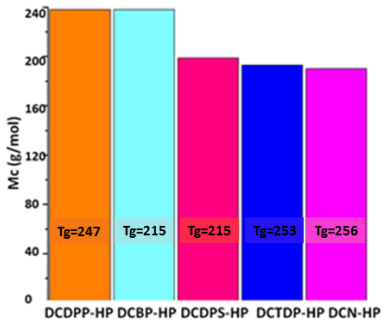

Fig. 3. Correlation study presenting molecular weight between the crosslinks (M_c) for the different cyanate ester homopolymers

Cyanate ester homopolymers show a range of M_c values from 198 g.mol^{-1} to 240 g.mol^{-1} (Fig. 3). DCN-HP has the lowest M_c value (198 g.mol^{-1}) following by DCTDP-HP, then DCDPS-HP, DCBP-HP, and DCDPP-HP (240 g.mol^{-1}). Those values depend on the planar structure of the aromatic ring and the ability of localized motions of chain segments [24]. In this reason, amongst the homopolymer systems, DCN-HP exhibits the lowest M_c value.

3.3. Fracture analysis

The cured homopolymers were subjected to SEM analysis to analyse the fractured surfaces. In general, the surfaces (Fig. 4) show similar, complex morphologies that are typical of shear

failure; all the polymers show elastic deformation zones that predominate. Previously, a commercial cyanate ester (AroCy B-30), which shares an identical chemical structure to DCDPP, was analysed using similar conditions.[25]

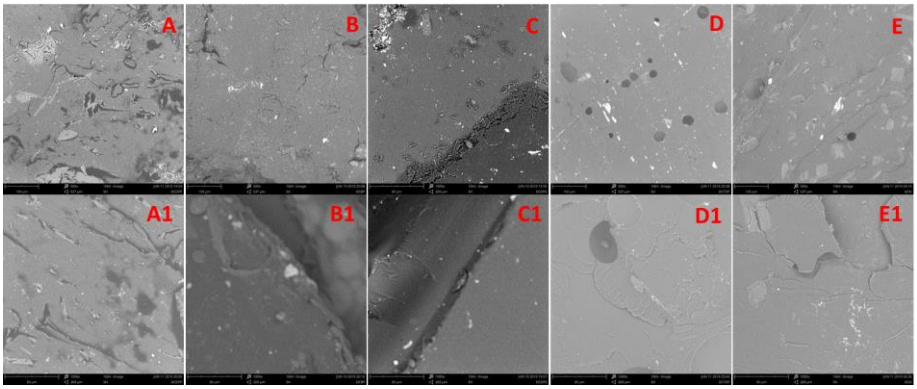

Fig. 4. Scanning electron microscopic images of the cured cyanate homopolymers with 500X (A-E) and 1000X (A1-E1) for DCDPP (A &A1), DCBP (B&B1), DCDPS (C&C1), DCTDP (D&D1), and DCN (E&E1)

3.4. Thermogravimetric analysis

3.4.1. Thermal properties

The thermal stabilities of the cured homopolymers were examined using the TGA technique: the thermal stability of polymers was evaluated by a number of parameters (Table 1) may lead to contradictory results, in terms of the onset temperature for degradation (DCDPP-HP), lowest rate of mass loss (DCN-HP), or highest char yield (DCN-HP and DCTDP-HP). The maximum decomposition temperature (MDT) is the temperature at which the highest rate of thermal degradation is recorded.

Table 1. Thermal properties of cyanate homopolymer

Polymer	Initial decomposition temperature IDT (°C)	Mass loss (%)			Maximum decomposition temperature MDT (°C)	Char residue at 800°C CR (%)
		3	15	30		
DCBP-HP	246	219	273	288	327	28
DCN-HP	229	196	260	274	264	35
DCTDP-HP	250	319	346	441	327	31
DCDPP-HP	388	411	434	446	438	16
DCDPS-HP	323	350	365	377	389	22

These data were not acquired using hyphenated apparatus in which chemical speciation was possible. Consequently, inferences are drawn based on the profile of the thermal degradation and comparisons of masses lost, with chemical moieties found within the polymer backbones. The TGA data for the homopolymers (Fig. 5a) suggests that, beyond the differences in onset temperatures, there are similarities in the degradation mechanism observed for DCBP-HP and DCTDP-HP. DCDPS-HP and DCDPP-HP both similarly lose mass in a single drop. The mass loss observed up to 150 ºC is probably due to the removal of water, which is used for recrystallization along with methanol.

DCN-HP shows the maximum decomposition temperatures all exceed 260 °C, and this occurs around 400 °C for the best performing systems (Fig. 5b), which contain sulphur in the backbone structure.

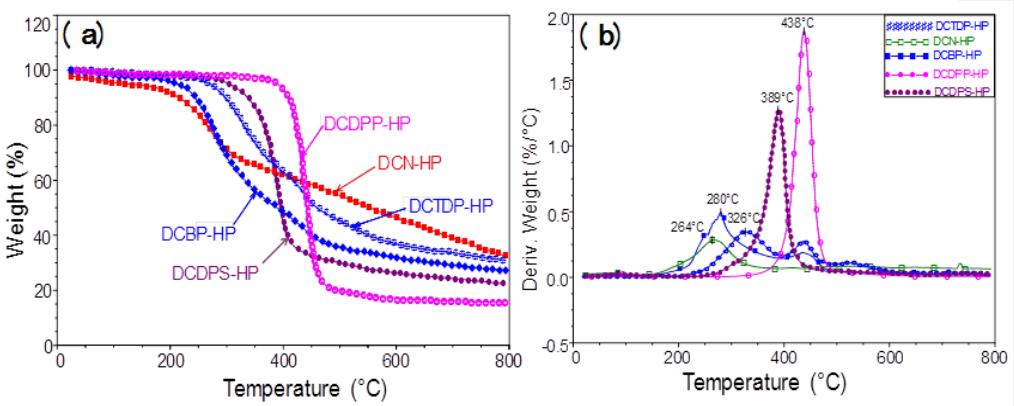

Fig. 5. TGA data (a) and DTG data (b) for the homopolymer systems carried out under N_2 atmosphere at a heating rate of 10°C/min.

The thermal decomposition of aromatic polycyanurates goes through a common mechanism which begins with thermolytic cleavage of the resin backbone and culminates with decyclization of the cyanurate rings around 300 °C, followed by char formation; these data are in good agreement with previous reports [26-28]. However, the other onsets can be attributed to two different species already present in the treated sample and not only formed during TGA execution, which showed the first onset around 450 ^{o}C corresponding to the decomposition into gaseous sulfonyl-di-benzene or propane-2,2-diyldibenzene unit. The char yields observed are typical for di-functional aromatic dicyanate homopolymers and DCN-HP, with the highest aromatic content, predictably shows the highest char yield (Table 1); DCDPP-HP with the greatest aliphatic character, the lowest. The flame-retardant property was found out from the limiting oxygen index (LOI) value, using the empirical formulae proposed by Van Krevelen *et al.* [29]. A numerical index, the LOI represents the minimum concentration of oxygen required to support the combustion of a polymer in the particular air mixture. Thus, higher LOI values represent better flame retardancy.

$$LOI = 17.5 + 0.4CR \quad (2)$$

where, *LOI* = limiting oxygen index, and *CR* = yield of char residue at 800ºC.

The homopolymer systems show the highest LOI values, which fall between 23-30, where values of LOI < 20.95, LOI < 28.0, and LOI <100 are considered to represent 'flammable', 'slow-burning', and 'intrinsically non-flammable' materials respectively (Fig. 6).

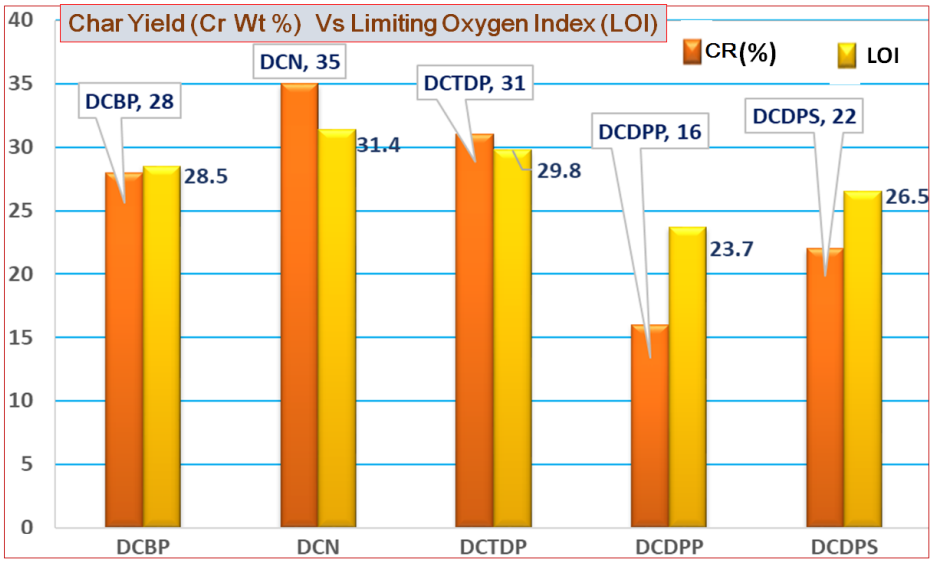

Fig. 6. The comparison of char yield *vs*. LOI to the cyanate system, the labelled (orange is CR (%), Yellow is LOI (%))

Using a more detailed description, the polymers possessing LOI ≥ 20.95 and ≥ 26.0 are considered as 'marginally stable' and 'self-extinguishable' materials, respectively [30-32]. According to these criteria, all the homopolymer systems (except DCDPP) have exhibited 'self-extinguishing' characteristics.

3.4. 2. Determination of activation energy

Thermogravimetric analysis was used for the determination of the kinetics of the thermal degradation of the polymers. The thermal degradation of the cured system was carried out at a heating rate of 10K min^{-1} under a flowing nitrogen atmosphere. The activation energy and order of reaction (n) were predicted by using the integral methods of the Broido, Horowitz-Metzger, and the Coats-Redfern models [3~~4~~-35] derived from the Arrhenius equation.

The basic equation used to describe decomposition reactions is

$$\frac{dy}{dt} = k(T)\,f(y) \qquad (3~~4~~)$$

where the rate constant $k(T)$ and $f(y)$ were functions of temperature, and conversion respectively was defined as

$$y = \frac{M_0 - M_t}{M_0 - M_f} \qquad (4~~5~~)$$

where M_0: initial sample weight, M_t and M_f were the weight at time t and final sample weight, respectively. Usually, k is assumed to follow the Arrhenius relationship:

$$k = A\exp\left(\frac{-E}{RT}\right) \qquad (6~~5~~)$$

The reaction rate may be written as follows.

$$\frac{dy}{dt} = \frac{dy}{dT}\frac{dT}{dt} = \beta\frac{dy}{dt} \qquad (7~~6~~)$$

Thus, change in mass *vs*. temperature can be written as

$$\frac{dy}{dT} = \frac{A}{\beta}\exp\left(\frac{-E_a}{RT}\right) f(y) \qquad (87)$$

The Coats-Redfern equation is as follows:

The integral form of Eq. 8 from initial temperature, T_i corresponding to a degree of conversion m_0, to a peak temperature, T_{max}, can be written as

$$\int_0^y \frac{dy}{f(y)} = \frac{A}{\beta}\int_{T_0}^{T_P} \exp\left(-\frac{E_a}{RT}\right) dT \qquad (98)$$

Using an approximation, Broido rearranged Eq (87).

$$\ln\left[\ln\frac{1}{y}\right] = -\frac{E_a}{R}\frac{1}{T} + \left(\frac{R}{E_a}\frac{A}{\beta}T_{\max}^2\right)_a \qquad (109)$$

$$\ln\left[\frac{-\ln(1-y)}{T^2}\right] = \ln\frac{AR}{\beta E_a}\left(1-\frac{2RT}{E_a}\right) - \frac{E_a}{RT} \quad \text{for } n = 1 \qquad (1110)$$

and the modified equation of Horowitz-Metzger is given by:

$$\ln(1-y) = \frac{E_a(T-T_P)}{R(T_P)} \quad \text{for } n = 1 \qquad (1211)$$

All of the models used give approximations since the decomposition of the systems involves several, often coincident or sequential reactions [26-28]. The Horowitz-Metzger model assumes a first-order reaction and uses the simplified exponential integrals to obtain the above equation. The Broido model considers the thermal decomposition process to be a first-order reaction. The Coats-Redfern model, when n = 1, was considered here for the activation energy calculations

[36]. The parameters used were: T is the absolute temperature, α is the conversion at temperature T, y is the fraction of initial molecules and not yet decomposed, T_{max} the absolute temperature of maximum reaction rate, β is the rate of heating, A is the frequency factor, DT_{max} is the maximum decomposition temperature, $\theta = T\text{-}DT_{max}$, R is the gas constant and E_a is the activation energy. A plot of ln(ln $1/y$) in case of Broido's method, In[$-(1-y)/T^2$] in case of Coats-Redfern method, and $(1-y)$ in the case of the Horowitz-Metzger method; *vs.* $1000/T$ for major degradation events yielded plots with linear portions. The changes in gradients are consistent with the different steps in the thermal degradation mechanism [26]. The cured samples of homopolymer systems were subjected to the kinetic analysis and are shown in Fig. 7, for the Horowitz-Metger model.

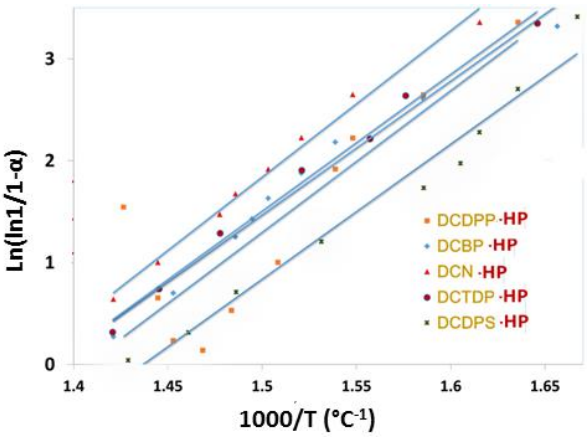

Fig. 7. The plots for the calculation of activation energies for homopolymers using the Horowitz-Metzger model

The kinetic parameters and the correlation coefficient (R^2) values of each system are summarized in Table 2.

Table 2 Comparison of kinetic parameters for the thermal degradation of the homopolymers using different models.

Polymer	Models					
	Broido		Horowitz-Metzger		Coats-Redfern	
	E_a (kJ.mol^{-1})	R^2	E_a (kJ.mol^{-1})	R^2	E_a (kJ.mol^{-1})	R^2
DCBP-HP	225	0.952	193	0.935	173	0.919
DCN-HP	173	0.970	159	0.964	140	0.953
DCTDP-HP	367	0.959	336	0.950	314	0.943
DCDPP-HP	223	0.933	190	0.899	163	0.866
DCDPS-HP	385	0.995	329	0.993	305	0.991

E_a = activation energy (kJ.mol-1); -R^2 = correlation coefficient.

While there are some differences in the activation energies (E_a) calculated, the trends observed are consistent between the different models and the E_a values were generally found to be in the following order for the models applied: Broido>Horowitz-Metzger>Coats-Redfern (Fig. 8). In the homopolymers, the E_a values derived using the Broido model fell between 173 - 385kJ/mol.

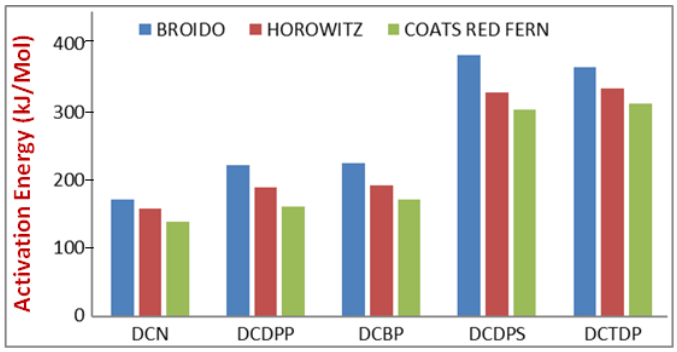

Fig. 8. Comparison of activation energies for the thermal degradation of the homopolymers using different models.

These values obtained for all the neat resins are higher than values that have previously been reported for the bisphenol E cyanate ester based on bisphenol E, 2,2'-bis(4-cyanatophenyl)ethylidene, (67 kJ mol^{-1}) [37] and a cyanate ester functional benzoxazine (100 kJ

277 mol^{-1}) [38] respectively. Within the data set, the highest activation energies calculated for the
278 thermal degradation of the homopolymers were obtained for the sulphur-containing
279 functionalized cyanate monomers (DCTP and DCDPS). The presence of sulphur plays a vital
280 role and the evolution of nonflammable gases (*e.g.* oxides of sulphur) during the degradation
281 may condense on the remaining polymer, thus diluting oxygen concentration at the polymer
282 surface, starving the flame, and serving as a free-radical flame front scavenger to inhibit
283 degradation of the polymers [39].
284
285
286 Five polycyanurate homopolymers displaying similar degrees of crosslink density, but
287 differing in terms of their molecular rigidity, were analysed for their thermal degradation
288 behavior, flame retardancy, and fracture properties. The homopolymers are all based on aromatic
289 monomers and so the high carbon content in the structure of homopolymers and presence of
290 nitrogen yields moderately high char yields (ranging from 16-35%, with DCDPP, containing an
291 aliphatic bridge, having the lowest value, and DCN, with no aliphatic character, the highest). The
292 activation energies (determined using the Broido model) for the decomposition behaviour of the
293 homopolymers revealed a wide variation, from 173 kJ/mol for DCN to 385 kJ/mol for DCDPS,
294 with the highest values in the data set being observed for homopolymers derived from simple
295 monomers.

296 **Acknowledgement:** One of the authors (MSL) would like to thank Dr. BSR Reddy, Retired
297 Emeritus Scientist, for his help and support. The author MSL also thank The CSIR-CLRI for the
298 financial support provided under MMP-06/18.

299

Formatted: Font color: Auto

REFERENCES

[1] Hamerton I., Hay J.N. *High Perform. Polym.*, 1998; 10(*2*): 163-174.

[2] Zhang Z., Liang G., Wang X., Adhikari S., Pei J., *High Perform. Polym.* 2013; 25: 427-435

[3] Fang T., Shimp D.A., *Prog. Polym. Sci.*, 1995; 20(*1*): 61-118

[4] Abed J.C., Mercier R., McGrath, J.E., *J. Polym. Sci. A Polym. Chem.* 1997; 35(*6*): 977-987

[5] Hamerton I. Chemistry and Technology of Cyanate Ester Resins. Glasgow: Blackie Academic; 1994

[6] Tao Q., Gan W., Yu Y., Wang M., Tang X., Li S. *Polymer*, 2004; 45(*10*): 3505–3510

[7] Anuradha G., Sarojadevi M., *J. Polym. Res*., 2008; 15(*6*): 507–514

[8] Fernandez A.M., Posadas P., Rodriguez A., Gonzalez L., *J Polym. Sci. A Polym. Chem*., 1999; 37(*16*): 3155-3168

[9] Laskoski M., Dominguez D.D., Keller T.M., *J. Polym. Sci. A Polym. Chem*., 2006; 44(*15*): 4559-4565

[10] Yan H.Q., Chen S., Qi G.R., *Polymer*, 2003; 44(*26)*: 7861-7867

[11] Pazhanikumar T., Sivasankar B., Sugumaran T., *High Perform. Polym*., 2007; 19(1): 97-112

[12] Bauer M., Bauer J., *J. Appl. Polym. Sci*., 2008; 110(*1*): 8–17

[13] Lin R.H., Hong J.L., Su A.C., *Polymer*, 1995; 36(*17*): 3349-3354

[14] Maya E.M., Snow A.W., Buckley L.J., *Macromolecules*, 2002; 35(*2*): 460-466

[15] Guenther A.J., Yandek G.R., Wright M.E., Petteys B.J., Quintana R., Connor D., *Macromolecules*, 2006; 39(*18*): 6046-6053

[16] Lin C.H., Yang K.Z., Leu T.S., Lin, C.H., Sie, J.W.., *J. Polym. Sci. A Polym. Chem*., 2006; 44(*11*): 3487-3502

[17] Abed J.C., Mercier R., McGrath J.E., *J. Polym. Sci. A Polym. Chem*., 1996; 35(*6*): 977-987

[18] Hamerton I, Emsley A.M., Howlin B.J., Klewpatinond P., Takeda S., *Polymer*, 2004; 45(*7*): 2193-2199

[19] Pankratov V.A., Vinogradova S.V., Korshak V.V., *Russ. Chem. Rev.*, 1977; 46(*3*): 278

[20] Lee J.Y., Jang J., *J. Polym Sci. A Polym. Chem.*, 1999; 37(*4*): 419-425

[21] Wang C.S., Lee M.C., *Polymer*, 2000; 4(*10*): 3631-3638

[22] Bauer R.S., *ACS Symp. Ser. Am. Chem. Soc*., Washington, DC, 1979; 114

[23] Zhavoronok E.S., Senchikhin I.N., Roldugin V.I, *Polym. Sci. Ser. A*, 2011; 53(*6*): 449.

[24] Lesser, A.J., Crawford, E., *J. Appl. Polym. Sci*., 1997; 66(2): 387-395.

[25] Hamerton, I. *High Perform. Polym*., 1996; 8(1): 83-95.

[26] Venkatesh M, Gouthaman S, Kanemoto S.O., Lakshmi M.S., Hamerton I., *J.Appl. Polym. Sci*. 2019; 136(*28*): 47754.

[27] Ramirez M.L., Walters R., Lyon R.E., Savitski E.P., *Polym. Degrad. Stab*., 2002; 78(*1*):73-82

[28] Lyon R.E., Walters R.N., Gandhi S., *Fire Mater*., 2006; 30(*2*): 89–106

[29] Van Krevelen D.W., *Polymer*, 1975; 16(*8*): 615–620

[30] Nelson M.I., *Combust. Theor. Model*., 2001; 5(*1*): 59-83

[31] Horrocks A.R., Price D., Tunc M., *J. Appl. Polym. Sci.*, 1989; 37(*4*): 1051-1061

[32] Fenimore C.P., In Flame-Retardant Polymeric Materials, New York: Plenum, 1975; 1: 371-397

[33] Doyle C.D., *Anal. Chem*., 1961; 33(*1*): 77–79

[34] Pashaei, S., Avval, M.M., Syed, A.A., *Chem. Ind. Chem. Eng. Quart*. 2011; 17(*2*): 141−151

[35] Holubka J.W., Devries J.E., Dickie R.A., *Ind. Eng. Chem. Prod. Res. Dev*., 1984; 23(*1*): 63-70

[36] Al-Mulla A., Shaban H.I., *Int. J. Polym. Mater*., 2008; 57(*3*): 275-287

[37] Muralidhara K.S., Sreenivasan S., *World Appl. Sci. J*., 2010; 11(2): 184-189

[38] Ashok M.A., Achar B.N., *Bull. Mater. Sci*., 2008; 31(*1*): 29-35

[39] Laufer G., Kirkland C., Morgan A.B., Grunlan J.C, *ACS Macro. Lett.*, 2013; 2(5): 361-365